View Online / Journal Homepage / Table of Contents for this issue
Dynamic Article Links

Nanoscale

Cite this: *Nanoscale*, 2012, **4**, 2306

www.rsc.org/nanoscale

PAPER

Conjugation of paclitaxel to iron oxide nanoparticles for tumor imaging and therapy

Dongfang Liu,[ab] Wei Wu,[c] Xi Chen,[a] Song Wen,[b] Xizhi Zhang,[a] Qi Ding,[a] Gaojun Teng[b] and Ning Gu*[a]

Received 5th December 2011, Accepted 26th January 2012
DOI: 10.1039/c2nr11918h

A strategy for conjugating an antitumor agent to superparamagnetic iron oxide nanoparticles (SPIONs) *via* a biocleavable ester binding is reported. Paclitaxel (PTX) was selected as a model drug. Both the *in vitro* and *in vivo* performance of the conjugates of SPION-PTX was investigated respectively. PTX can be released slowly through the hydrolysis of the ester bond in a pH-dependent manner and the SPION-PTX has near equal cytotoxity to the clinical PTX injection (Taxol) at the equivalent dose of PTX. Furthermore, the SPION-PTX can accumulate in tumor tissues as demonstrated by MRI and exhibit better tumor suppression effect than Taxol *in vivo*. The above good performance of the SPION-PTX together with the good biocompatibility of the SPIONs would promote greatly the application of the SPIONs in the biomedicine field.

Introduction

Superparamagnetic iron oxide nanoparticles (SPIONs) have been attracting considerable research interests in developing effective drug delivery systems due to their simple, scalable preparation, specific magnetic properties and good biocompatibility. Comparing to other nano drug delivery systems, such as polymeric nanoparticles,[1] liposomes[2] and micelles,[3] SPIONs possess magnetic resonance imaging (MRI) enhancement properties,[4–6] which potentially makes it possible to monitor drug distribution in real-time and follow the effect of therapeutics on the progression of the disease. In addition, SPIONs are biodegradable, which benefits greatly their biomedical applications.[7] However, the efficacy of SPIONs as nanovehicles for drugs is often compromised by the quick opsonization of SPIONs and subsequent plasma clearance by tissue macrophages of the reticuloendothelial system (RES) prior to reaching the target tissue or cells.[8] Surface modification with nonfouling polymers, such as pluronic F-127[9] and polyethylene glycol (PEG) derivatives,[10] is a direct and effective way to address this issue. By doing so, the blood-circulation time can be significantly increased by minimizing or eliminating the protein adsorption to the nanoparticles. The prolonged blood-circulation time highly favors the tumor accumulation of the SPIONs *via* the enhanced permeability and retention (EPR) effect and can be employed in drug delivery. Yu *et al.* loaded doxorubicin *via* electrostatic interactions to the poly(TMSMA-r-PEGMA)-coated, thermally cross-linked superparamagnetic SPIONs (TCL-SPIONs). The Dox-loaded TCL-SPION exhibited excellent *in vivo* antitumor effects due to the passive tumor targeting efficiency of the TCL-SPION carriers. However, the drug loading of this system is quite low (2 wt%).[11]

Very recently, we have reported the synthesis of PEGylated SPIONs (SPION-PEG) which can effectively resist the RES uptake and accumulate in tumor tissue *via* the EPR effect without the aid of targeting ligands.[12] Encouraged by the good passive targeting ability to the tumor of the SPION-PEG, we hypothesized that it could deliver anticancer drugs to tumor sites with high efficiency. Herein, we present a strategy for covalently conjugating an antitumor agent to the SPION-PEG and investigate the *in vivo* behavior and therapeutic effect of the obtained nanomedicine. Paclitaxel (PTX) was selected as a model drug and linked to SPION-PEG *via* a biocleavable ester linkage (Scheme 1). PTX has a prominent therapeutic role to a broad spectrum of tumors by interacting with microtubules.[13] However, the inherent poor solubility of PTX in aqueous medium greatly limits its clinical applications. As the SPION-PEG has good solubility in aqueous solution and a good passive targeting ability to the tumor, we anticipate that combining PTX with SPION-PEG through a biocleavable linking manner can improve the aqueous solubility and tumor enrichment of the drug.

Experimental

1. Synthesis and characterization

1.1 Materials. Poly(acrylic acid) (PAA, Mw ≈ 1,800), *N*-(3-dimethylaminopropyl)-*N*′-ethylcarbodiimide hydrochloride (EDC·HCl) and *N*-hydroxysuccinimide (NHS) were purchased

[a]*Jiangsu Key Laboratory for Biomaterials and Devices, State Key Laboratory of Bioelectronics, School of Biological Science and Medical Engineering, Southeast University, Nanjing, 210096, China. E-mail: guning@seu.edu.cn; Fax: +86-025-83272460; Tel: +86-025-83272476-8888*
[b]*Laboratory of Molecular Imaging, School of Medicine, Southeast University, Nanjing, China 210096*
[c]*Laboratory of Mesoscopic Chemistry and Department of Polymer Science & Engineering, College of Chemistry & Chemical Engineering, Nanjing University, Nanjing, 210093, China*

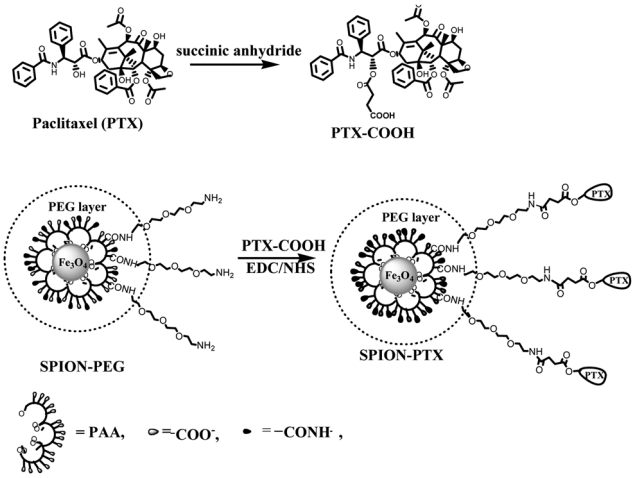

Scheme 1 Schematic chemical structures of PTX-COOH, SPION-PEG, SPION-PTX and their synthetic routes.

from Sigma-Aldrich. α,ω-Diamino PEG (Mw ≈ 3,350) was purchased from Biomatrik Inc. PTX was purchased from Nanjing Zelang Medical Technology Co. Ltd, and was modified by succinic anhydride according to the literature, adding a carboxyl acid group on the molecule at the C–2′–OH position to give PTX-COOH.[14] Clinical Taxol paclitaxel injection was purchased from Bristol-Myers Squibb Company. The SPION-PEG was synthesized by a two-step method reported elsewhere.[12]

1.2 Synthesis of SPION-PTX. A solution of PTX-COOH (2 mg, 0.002 mmol) in 0.2 mL of anhydrous DMSO was activated with EDC·HCl (15 mg, 0.08 mmol) and NHS (10 mg, 0.09 mmol) for 1 h and subsequently added to a solution of SPION-PEG (containing of 8 mg of iron) in 0.8 mL of anhydrous DMF. The resulting mixture was stirred at room temperature overnight. Thereafter, the product was purified by dialysis against water for 2 h and then ultrafiltration with ultra-4 centrifugal filter devices (Millipore's Amicon, 100 000 NMWL) to remove the impurity substances. The purification was monitored by testing the filtrate with TLC visualized by iodine vapor.

1.3 Characterization. UV-Vis spectra were performed on a Shimadzu UV-3600 spectrophotometer. Transmission electron microscopy (TEM) analysis was carried out on a JEM-2000EX microscope. The hydrodynamic diameter and size distribution of the prepared SPIONs were determined by dynamic light scattering (DLS) using a Brookhaven BI9000AT system (Brookhaven Instruments Corp.). The zeta potential of the samples were obtained with Zetaplus (Brookhaven Instruments Corp.). Magnetic properties were determined with a vibrating sample magnetometer (VSM, Lakeshore 7407) at room temperature in a field up to 10 kOe.

1.4 Drug loading in the SPIONs. To determine the amount of PTX loaded in SPION-PTX, a standard linear-fit curve of free PTX in ethanol was created by plotting the UV-Vis absorbance at 227 nm of several PTX ethanol solutions with known concentrations. The concentration of PTX in SPION-PTX was determined by subtracting out the background absorbance of a sample of SPION-PEG with a normalized amount of iron at 277 nm.

2. Cell toxicity assay

Hela cells were seeded in 96-well plates at 5×10^3 cells/well and were allowed to adhere overnight. The growth medium was replaced with a fresh one containing varying concentrations of SPION-PTX, SPION-PEG and Taxol. Cells were then incubated for 24 h and washed three times by 1 mL PBS. Subsequently, cells were incubated in a growth medium containing 1 mg mL^{-1} MTT agent for an additional 4 h at 37 °C and 500 μL of DMSO was added to each well to ensure the solubilization of formazam crystals. Each concentration of the samples was repeated three times. The optical density (OD) of the solution was measured with a microplate reader at 570 nm.

3. *In vitro* release of SPION-PTX in buffer solution

A predetermined amount of SPION-PTX was dispersed in 0.5 mL of release medium with a specific pH value (phosphate buffered saline (pH = 7.4, 0.1 M) and acetate buffered saline (pH = 5.0, 0.1 M)). The resulting solution was dialyzed against 20 mL of the corresponding release medium (containing 0.1% v/v Tween 80) in a 3350 Da MWCO membrane at 37 °C with gentle agitation for 72 h. At predetermined time intervals, aliquots (1 mL) were taken from the outer medium and then the same volume of fresh medium was replenished immediately. The parts taken out were stored at −20 °C until analysis by HPLC. Chromatographic separation was achieved using a HC-C18 column (250 × 4.6 mm, 5 μm, C18, Agilent Technologies, Palo Alto, USA) at 35 °C. The mobile phase consisted of 42 : 58 double-distilled water (Milllipore, Milford, USA)/acetonitrile (HPLC grade, Merck). The flow rate was set to 1.0 mL min^{-1} and UV detection wavelength was 228 nm. The concentration of PTX was determined based on the peak area at the retention time of ~7.3 min by reference to a calibration curve.

4. *In vivo* MR imaging

The tumor models were established by inoculating subcutaneously H22 tumor cells (5–6 × 10^6 cells per mouse) into the proximal thigh region of ICR mice (6–8 weeks, 22–26 g). MR images were taken prior to the injection of SPION-PTX and at appropriate time points post-injection. Mice were anaesthetized for imaging with isoflurane (1.5% vol. at 2 L min^{-1}) *via* a nose cone. Body temperature was maintained at 37 °C. SPION-PTX in saline solution was injected intravenously through the tail vein. The *in vivo* MRI experiment was performed on mice with the use of a 3.8 cm circular surface coil in transmit/receive mode conducting on 7 Tesla Micro-MRI (PharmaScan, Brukers, Germany). MR imaging of mice was performed with T2* flash sequence. The parameters were TR/TE = 408 ms/3.5 ms, flip angle = 30°, FOV = 35 mm × 35 mm, slice thickness = 1 mm, matrix 256 × 256.

5. *In vivo* tumor inhibition of SPION-PTX

All animal experiments were performed in compliance with guidelines set by the Animal Care Committee of the Southeast

University. To establish the experimental model of the tumor, H22 tumor cells (5–6 × 10^6 cells per mouse) were inoculated subcutaneously into the armpit of ICR mice (6–8 weeks, 22–26 g). When the tumor reached a mean volume of ~300 mm^3 (6 days after inoculation), the mice were randomly divided into four groups (six per group) and then injected *via* the tail vein with a 0.3 mL solution of different formulations of PTX (SPION-PTX and clinical taxol injection), SPION-PEG in saline and neat saline (0.3 mL, as negative control), respectively. Both of the formulations of PTX were injected with the dose normalized to be 5 mg kg^{-1} PTX equiv, respectively. The injection of SPION-PEG contains the same amount of iron as the SPION-PTX (about 30 mg kg^{-1} of iron). After the administration, 7 day follow-up experiments were performed, in which tumor sizes were measured by a vernier caliper on an alternate day and calculated as volume $V = d^2 \times D/2$ (where d and D denote the shortest and longest diameter of the tumor in mm, respectively), and the weights and clinical situations of all the tested mice were also scrutinized.

The tumor growth inhibition (*TGI*) was calculated by the following equation:

$$TGI = \frac{\overline{V} \text{ of saline control group} - \overline{V} \text{ of tested group}}{\overline{V} \text{ of saline control group}} \times 100\%$$

Where $\bar{V}$ means the average of tumor volume.

Statistical analysis: Student's *t*-test was used to determine the difference of tumor inhibition between the groups treated with SPION-PTX and PTX injection at the equivalent dose of PTX, and P values less than 0.05 were considered statistically significant.

Results and discussion

The preparation of SPION-PTX is shown schematically in Scheme 1. To couple PTX with SPIONs, a succinate-based PTX ester derivative (PTX-COOH) was initially synthesized following the published procedures.[11] Thereafter, the PTX-COOH was activated with EDC·HCl and NHS and then attached to the surface of SPION-PEG *via* amidation, affording SPION-PTX (Scheme 1). After the removal of the unconjugated PTX-COOH by dialysis and ultrafiltration, the specific linkage of PTX to SPIONs was confirmed by the UV-vis spectrum (Fig. 1a). The appearance of a shoulder peak at 227 nm, which is the characteristic of PTX, indicates the successful conjugation of PTX to SPIONs. Actually, the spectrum of the SPION-PTX can be looked as superposing the spectra of SPION-PEG and PTX since the curve obtained by subtracting the spectrum of SPION-PEG from that of the SPION-PTX is well consistent with the spectrum of PTX (Fig. 1a). Upon subtraction of the contribution of SPION-PEG to the spectrum of SPION-PTX, the loading of PTX can be determined to be ~15 wt% (PTX/Fe) by measuring the absorbance at 227 nm and using a preestablished calibration curve.

The SPION-PTX has good solubility in aqueous medium. The average diameter of the SPION-PTX conjugates was determined to be ~10 nm by TEM and no obvious aggregation can be detected (Fig. 1b). Fig. 1c shows the hydrodynamic size distribution of the SPION-PTX measured by DLS. The mean

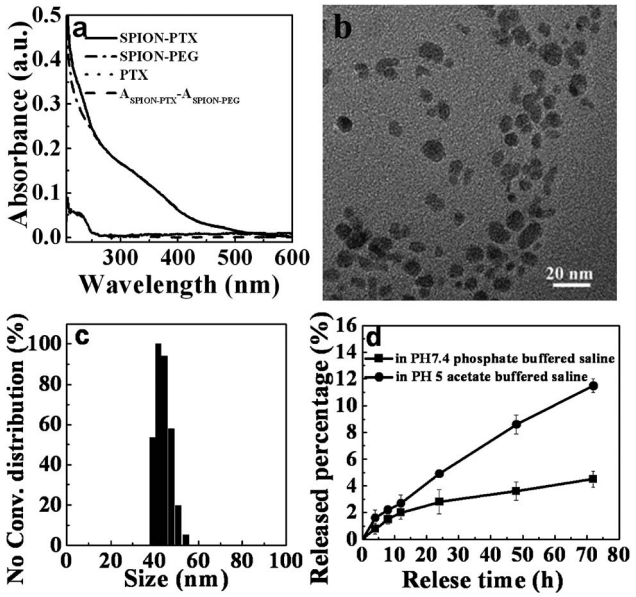

Fig. 1 (a) UV-Vis spectra of SPION-PTX, SPION-PEG, PTX in ethanol and the curve obtained by subtracting the spectrum of SPION-PEG from that of the SPION-PTX. (b) Typical TEM image of SPION-PTX. (c) Hydrodynamic diameter distribution of SPION-PTX in distilled water. (d) *In vitro* release profiles of SPION-PTX in the media of phosphate buffered saline (pH 7.4, 0.1 M, square), acetate buffered saline (pH 5.0, 0.1 M, circle) at 37 °C, expressed as the percentage of cumulative release to the total amount of PTX in the sample.

diameter of SPION-PTX in water is ~45 ± 2.6 nm with a polydispersity index (PDI) of 0.29.

For the application of SPIONs in MR imaging, it is pivotal that SPIONs retain their magnetic properties after the modification treatments. Fig. 2 shows the VSM of the SPION-PTX with SPION-PEG as a control. It can be observed that the attachment of PTX has negligible effect on the hysteresis loops of the SPIONs, that is to say, the SPIONs retain their superparamagnetic character after the attachment of PTX and the saturation magnetization (73 emu/g Fe) of SPION-PTX is similar to that of SPION-PEG.

Since the ester bond used to link the SPION and drug moieties is hydrolytically unstable, the SPION-carried PTX should be released in an aqueous environment to some extent. Fig. 1d shows the *in vitro* PTX release profiles of SPION-PTX sample in the media with different pH values. It can be seen that PTX release is faster at pH 5.0 than pH 7.4 within a 72 h monitoring duration. However, the released portion did not exceed 15% of the total amount of loaded drug during the experiment period at either pH 5.0 or 7.4, indicating relatively high stability of the ester bond in buffer solutions.

To examine the pharmacological activity of SPION-PTX and the potential toxicity of the SPION carrier, the *in vitro* cytotoxicity of SPION-PTX and SPION-PEG against HeLa cells was investigated together with a positive control of clinical PTX injection (Taxol) (Fig. 3). The inhibitory ratio was determined after 24 h of incubation with a series of doses of PTX injection, SPION-PTX or SPION-PEG by MTT assay. As shown in Fig. 3a, SPION-PTX exhibit similar toxicity as Taxol (Fig. 3a) without any loss of cancer cell destruction ability. No detectable

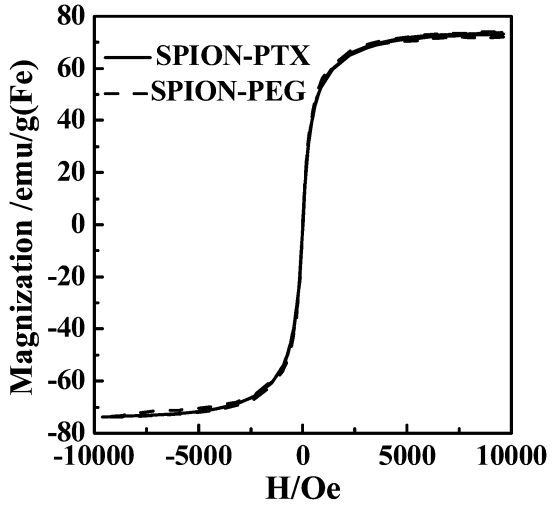

Fig. 2 Variation of the magnetization of SPION-PTX (solid line) and SPION-PEG (dashed line) as a function of applied magnetic field.

toxicity was observed for SPIONs carriers at all used concentrations (Fig. 3b).

We next examined the ability of SPION-PTX to accumulate in tumor tissues *via* the EPR effect. Tumor-bearing mice were prepared by subcutaneous injection of the hepatic H22 cells into the proximal thigh region of mice, and then MR imaging of the mice was conducted at pre-injection and various time points post-injection of SPION-PTX (8 mg kg^{-1}). Before injection of SPION-PTX, the tumor appears as a hyperintense area in T2*-weighted MR images (indicated by white arrow in Fig. 4a). At 4 h post-injection, the relative signal decrease (*RSD* %) in the tumor (indicated by white arrow in Fig. 4b) of the T2*-weighted MR images was calculated to be ~32% with respect to pre-injection, indicating accumulation of the SPIONs in the tumor. The value of *RSD* in the tumor for SPION-PTX is slightly lower than that for the SPION-PEG (RSD: ~45%),[12] which may be caused by the high hydrophobicity of the conjugated PTX that shorten the blood circulation time.

The *in vivo* antitumor performance of SPION-PTX was further investigated by using subcutaneous hepatic H22 tumor bearing ICR mice as the model animals and was compared with the clinical Taxol formulation with the dose normalized to be 5 mg of PTX equivalent (equiv) per kilogram of body weight, respectively. SPION-PEG (containing the same SPION concentration as SPION-PTX with a dose of 5 mg kg^{-1} PTX equiv) and saline-treated groups were used as controls. All of the samples were injected as a solution in 0.3 mL of saline. Seven day follow-up experiments were carried out after administrations. Both the two PTX formulations (SPION-PTX and Taxol injection) exhibit dose-dependent antitumor features, that is, the

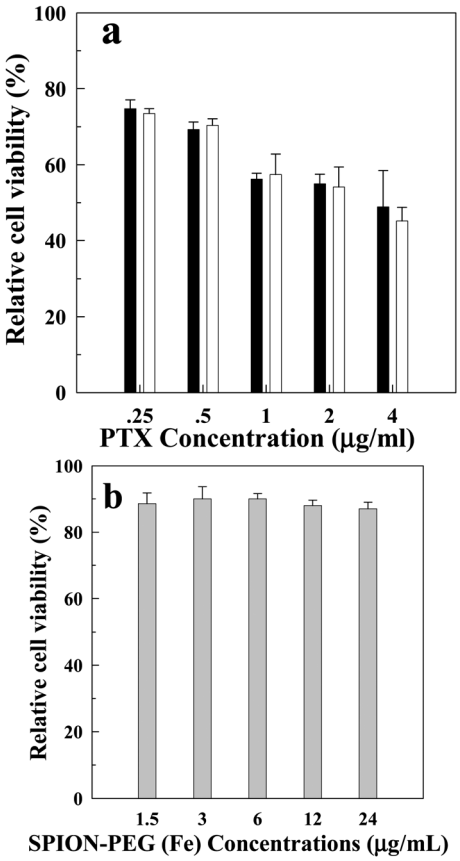

Fig. 3 *In vitro* cytotoxicity of clinical PTX injection (a, black), SPION-PTX (a, white), and SPION-PEG (b, contains the same amount of iron as the SPION-PTX) against Hela cells.

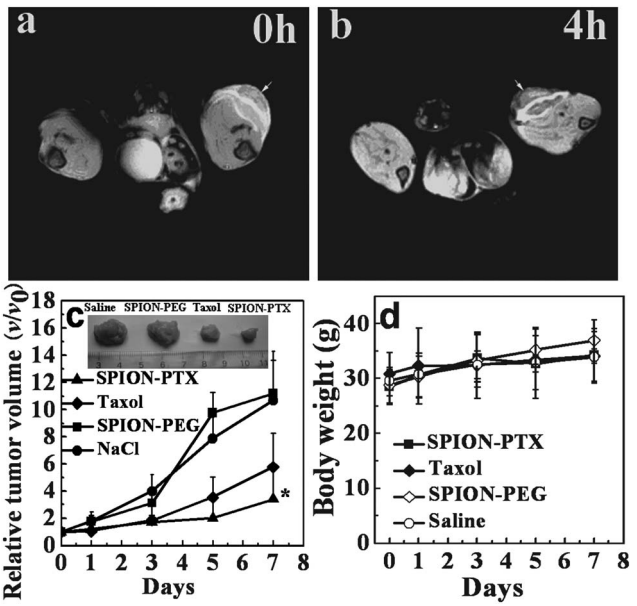

Fig. 4 T2*-weighted images (TR/TE of 408 ms/3.5 ms) at pre-injection (a) and 4 h post-injection (b) of 8 mg kg^{-1} of SPION-PTX at the level of the tumor on the proximal thigh of the mice. The white arrow indicates the tumor region. (c) *In vivo* antitumor effect obtained from each treated group, expressed as the average values of the relative tumor volume $v/v0$ (where v denotes the tumor volume at test time points and $v0$ denotes the corresponding initial tumor volume at the beginning of treatment). $^*P < 0.05$ (*versus* PTX injection group at the equivalent dose from the 5th day). Inset shows the typical photographs of excised tumors from mice on the 7th day after treatments with SPION-PTX (5 mg kg^{-1} equiv), PTX (Taxol) injection (5 mg kg^{-1} equiv), SPION-PEG and saline. (d) Evolution of body weight of each group during the experiments. Data in (c) and (d) are presented as mean ± SD (n = 3–5).

higher the drug dose, the better antitumor activity (Fig. 4c). The tumor growth inhibition (*TGI*) calculated for the group treated with SOPIN-PTX at the doses of 5 mg kg^{-1} PTX equiv is 68% on the 7th day (see Experimental for the calculation method). By contrast, the *TGI* obtained from the group treated with Taxol injection at dose of 5 mg kg^{-1} PTX equiv is 46%, much lower than that of the group treated with SPION-PTX. In addition, it is also found that SPION-PEG has negligible inhibition effect. The distinct inhibition effects can also be illustrated by the intuitive evidence from the representative photographs of excised tumor tissues (inset Fig. 4c). Over the course of the study, the weights (Fig. 4d) and clinical situations of all the tested groups were scrutinized, and neither mortality nor noticeable body weight loss of the mice treated with either of the two formulations of PTX or SPION-PEG was observed compared with the saline-treated group, indicating the well-tolerated dose levels of drug and the negligible toxicity of SPIONs imposed on the experimental mice.

Conclusions

In conclusion, a strategy for conjugating an antitumor agent to SPIONs is developed. In this strategy, PTX was covalently linked to SPIONs *via* a biocleavable ester binding. The SPION-PTX is characterized by UV-Vis, TEM, DLS and VSM respectively. *In vitro* experiment demonstrated that PTX can be released slowly through the hydrolysis of the ester bond in a pH-dependent manner and the SPION-PTX have equal cytotoxity to the clinical PTX injection (Taxol) at the equivalent dose of PTX. Furthermore, the SPION-PTX can accumulate in tumor tissues as demonstrated by MRI and exhibit better tumor suppression effect than Taxol. The above good performance of the SPION-PTX together with the good biocompatibility of the SPIONs would promote greatly the application of the SPIONs in biomedicine field.

Acknowledgements

This investigation was supported by the National Important Science Research Program of China (Nos. 2011CB933500, 2011CB933503), the National Natural Science Foundation of China (Nos. 81101139) and the Basic Research Program of Jiangsu Province (Natural Science Foundation) (Grant Nos. BK2009013, BK2010303)

Notes and references

1 L. Zhang, Y. Lin, J. Wang, W. Yao, W. Wu and X. Jiang, *Macromol. Rapid Commun.*, 2011, **32**, 534–539.
2 R. Tarallo, A. Accardo, A. Falanga, D. Guarnieri, G. Vitiello, P. Netti, G. D'Errico, G. Morelli and S. Galdiero, *Chem.–Eur. J.*, 2011, **17**, 12659–12668.
3 C. K. Huang, C. L. Lo, H. H. Chen and G. H. Hsiue, *Adv. Funct. Mater.*, 2007, **17**, 2291–2297.
4 D. Artemov, *J. Cell. Biochem.*, 2003, **90**, 518–524.
5 K. Park, S. Lee, E. Kang, K. Kim, K. Choi and I. C. Kwon, *Adv. Funct. Mater.*, 2009, **19**, 1553–1566.
6 R. Qiao, C. Yang and M. Gao, *J. Mater. Chem.*, 2009, **19**, 6274–6293.
7 N. Sanvicens and P. Marco, *Trends Biotechnol.*, 2008, **26**, 425–433.
8 A. Q. Pankhurst, J. Connolly, S. K. Jones and J. Dobson, *J. Phys. D: Appl. Phys.*, 2003, **36**, R167–R181.
9 T. K. Jain, J. Richey, S. Michelle, D. L. Leslie-Pelecky, C. A. Flask and V. Labhasetwar, *Biomaterials*, 2008, **29**, 4012–4021.
10 J. R. Hwu, Y. S. Lin, T. Josephrajan, M. H. Hsu, F. Y. Cheng, C. S. Yeh, W. C. Su and D. B. Shieh, *J. Am. Chem. Soc.*, 2009, **131**, 66–68.
11 M. K. Yu, Y. Y. Jeong, J. Park, S. Park, J. W. Kim, J. J. Min, K. Kim and S. Jon, *Angew. Chem., Int. Ed.*, 2008, **47**, 5362–5365.
12 D. F. Liu, W. Wu, J. J. Ling, S. Wen, N. Gu and X. Z. Zhang, *Adv. Funct. Mater.*, 2011, **21**, 1498–1504.
13 V. Vassileva, C. J. Allen and M. Piquette-Miller, *Mol. Cancer Ther.*, 2008, **7**, 630–637.
14 H. M. Deutsch, J. A. Glinski, M. Hernandez, R. D. Haugwitz, V. L. Narayanan, M. Suffness and L. H. Zalkow, *J. Med. Chem.*, 1989, **32**, 788–792.

